European Radiology
https://doi.org/10.1007/s00330-020-06882-x

UROGENITAL

MRI-directed high-frequency (29MhZ) TRUS-guided biopsies: initial results of a single-center study

François Cornud[1,2] · Arnaud Lefevre[1] · Thierry Flam[3] · Olivier Dumonceau[4] · Marc Galiano[5] · Philippe Soyer[2,6] · Philippe Camparo[7] · Matthias Barral[2]

Received: 7 January 2020 / Revised: 25 February 2020 / Accepted: 9 April 2020

Abstract

Objectives To evaluate the ability of high-frequency (29 MHz) transrectal micro-ultrasound (microUS) as a second-look examination after biparametric MRI (bp-MRI) and to reidentify focal lesions seen on diagnostic MRI and to detect new ones

Methods A total of 118 consecutive men (mean age, 66 ± 13 [SD] years; range, 49–93 years) with a mean prostate-specific antigen level of 11 ± 19 (SD) ng/mL (range, 2–200 ng/mL) and at least one focal lesion (MRI+) with a score > 2 on bp-MRI were included. Of these, 79/118 (66.9%) were biopsy-naïve and 102/118 (86.5%) had non-suspicious rectal examination. All patients had MRI-directed microUS-guided biopsy using a 29-MHz transducer. All lesions visible on micro-ultrasound (microUS+) were targeted without image fusion, which was only used for MRI+/microUS− lesions. Significant prostate cancer (sPCa) was defined by a Gleason score ≥ 7 or a maximum cancer core length > 3 mm.

Results A total of 144 focal prostatic lesions were analyzed, including 114 (114/144, 79.2%) MRI+/microUS+ lesions, 13 MRI+/microUS− lesions (13/144, 9%), and 17 MRI−/microUS+ lesions (17/144, 11.8%). Significant PCa was detected in 70 MRI+/microUS+ lesions (70/114, 61.4%), in no MRI+/microUS− lesion (0/13, 0%), and in 4 MRI-/microUS+ lesions (4/17, 23.5%). The sensitivity and specificity of microUS on a per-patient and a per-lesion basis were 100% (95% CI, 84.9–100%) and 22.8% (95% CI, 12.5–35.8%) and 100% (95% CI, 85.1–100%) and 22.6% (95% CI, 12.3–36.2%), respectively.

Conclusion MicroUS, as a second-look examination, may show promise to localize targets detected on bp-MRI.

Key Points

- *Used as a second-look examination, microUS-guided biopsies have a 100% detection rate of sCa originating in the PZ or lower third of the TZ, without microUS-MRI image fusion.*
- *MicroUS results may provide additional information about lesions visible on MRI.*
- *MicroUS may provide the ability to detect small PZ lesions undetected by bp-MRI.*

Keywords Ultrasonography · Prostatic neoplasms · Biopsy · Magnetic resonance imaging

Abbreviations

ADC	Apparent diffusion coefficient
bp-MRI	Biparametric MRI
DCE	Dynamic contrast-enhanced
DWI	Diffusion-weighted imaging
FTB	Fusion targeted biopsies
MRI	Magnetic resonance imaging
PCa	Prostate cancer
PSA	Prostate-specific antigen
PZ	Peripheral zone

✉ François Cornud
francois.cornud@imagerietourville.com

Olivier Dumonceau
dr.dumonceau@gmail.com

[1] Department of Radiology, Clinique de l'Alma, Paris, France

[2] Department of Radiology, Hôpital Cochin, Assistance Publique Hôpitaux Paris, AP-HP, Paris, France

[3] Department of Urology, Clinique St Jean de Dieu, Paris, France

[4] Department of Urology, Clinique Turin, Paris, France

[5] Department of Urology, Clinique de l'Alma, Paris, France

[6] Université de Paris Descartes Paris V, Paris, France

[7] Centre de Pathologie, Amiens, France

Published online: 29 April 2020

TRUS Transrectal ultrasound
TZ Transition zone

Introduction

The PRECISION trial has demonstrated that a targeted biopsy strategy, applied only in men with suspicious findings on MRI, detected more significant prostate cancers (PCa) than transrectal systematic biopsies [1]. These results suggest that prostate MRI will increasingly be performed prior to biopsy [2] and that a targeted-biopsy-only strategy, although questioned by some authors [3, 4], may become the reference standard [5–9].

Two approaches for transrectal targeted biopsy based on MRI findings are available. In the first, the MRI findings are superimposed on the real-time transrectal ultrasound (TRUS) during biopsy, either cognitively or using a software-based TRUS-MRI image-fusion system [10]. However, this fusion-guided targeted biopsy (FTB) technique conveys, even in experienced hands, several limitations including motion of patient/prostate during biopsy [11] and registration mismatch inherent to the computational constraints of software-based systems [12]. These limitations may lead to targeting errors, especially for smaller and more anterior lesions (long axis < 15 mm) [8].

The second approach to leverage MRI findings is in-bore MRI-guided biopsy. This technique is accurate because the same imaging modality is used to localize and sample the lesion, which eliminates cross-modality registration errors [13]. In addition, the use of robotic assistance shortens the examination time compared to manual positioning [14]. In-bore MRI-guided biopsy is suitable for anterior lesions which are rarely visible on conventional TRUS. In-bore guidance suffers from a limited availability of interventional MRI, due to the cost of the disposable materials and the required time in the MRI room. It should thus be used only in selected indications [14].

To overcome the limitations of both MRI-TRUS image fusion and in-bore MRI guidance would require a real-time, accessible imaging modality with a higher resolution than conventional TRUS. Micro-ultrasound (microUS) is a new imaging modality, which uses a linear TRUS probe working at high frequency (29 MHz). The acquired images have a resolution of up to 70 μm and initial results are promising [15–18].

The primary objective of this study was to evaluate the value of high-frequency (29 MHz) microUS, as a second-look examination, to visualize foci detected by MRI, and perform targeted TRUS-guided biopsies. The secondary objective was to determine if microUS could detect lesions not visible on MRI.

Materials and methods

Patients

This single-center study was approved by our Institutional Review Board, and informed consent was waived. From February to June 2019, 118 consecutive patients with an elevated or rising PSA level and at least one focal abnormality with a biparametric MRI score > 2 were included. Clinical characteristics of the 118 patients are presented in Table 1.

MRI protocol

MRI examinations were performed with a 1.5-T unit (Aera, Siemens Healthineers) equipped with 64 radiofrequency/RF receiver channels and a pelvic phased array coil with 60 elements. This setup provides a sufficient signal-to-noise ratio so that an endorectal coil is not required [19]. MRI parameters of our biparametric protocol are shown in Table 2. For the transition zone (TZ), the bp-MRI score was similar to the multiparametric MRI score defined by PI-RADS v2, since the dynamic contrast-enhanced (DCE) MRI sequence is not typically used in this region. For the peripheral zone (PZ), the diffusion-weighted imaging (DWI) score was calculated as described elsewhere [20] by measuring the ratio of the mean ADC value of foci to that of the rest of the prostate including the PZ and the TZ. An ADC ratio ≥ 0.68 indicated mild restricted diffusion, and a bp-MRI score of 3 was assigned. In patients with an ADC ratio < 0.68, a bp-MRI score of 4 was assigned. High computed *b* values, 2000 and 4000 s/mm^2 in the vast majority of cases and occasionally 6000 s/mm^2, calculated with a commercially available software (Olea Sphere, Olea Medical) were used to optimally increase the conspicuity of tumor foci originating in the PZ [20, 21] as well as in the TZ, as reported previously [22]. MR images were displayed on a workstation placed close to the TRUS screen for review during the biopsy procedure.

Table 1 Clinical characteristics of the 118 patients

Naïve biopsy patients	79/118 (67%)
Repeat biopsy patients	39/118 (33%)
Previous negative biopsy	32/39 (82%)
Active surveillance	7/39 (18%)
Mean age (years)	66 ± 13 [49–93]
Non-suspicious rectal examination	102/118 (86.5%)
Mean PSA serum level (ng/mL)	11 ± 19 [2–200]
Prostate volume (ellipsoid formula*, cm^3)	53 ± 26 [16–180]

Quantitative variables are expressed as means ± standard deviations; numbers in brackets are ranges. Qualitative variables are expressed as proportions; numbers in parentheses are percentages

*Width × height × length × Π/6

Table 2 MRI protocol with a pelvic phased array coil with 60 elements

	TR (ms)	TE (ms)	Slice thickness (mm)	Matrix size	FOV	*b* values (s/mm^2)
T2-weighted	2810	163	3	179 × 256	135 × 35	n.a.
DWI	4100	71	3	95 × 100	200 × 200	50/500/1000* 2000/4000/6000**

FOV field of view, *DWI* diffusion-weighted imaging, *n.a.* not applicable

*Acquired *b* values for the ADC map

**Computed *b* values

High-frequency TRUS protocol

All patients underwent a high-frequency TRUS examination with a 29-MHz linear transducer (ExactVu, Exact Imaging). This device enables a real-time spatial resolution of 70 μm which represents a threefold improvement in resolution compared with conventional 9–12-MHz TRUS probes. Higher-frequency ultrasound is normally associated with a decrease in penetration and limited imaging depth. The ExactVu system incorporates a range of technological advances in both transducer fabrication and image processing, which allows the 29-MHz system to achieve an acceptable signal-to-noise ratio at a depth of 5 cm, instead of the 3 cm normally associated with these frequencies. These advances produce ultrasonic crystals with an extremely wide bandwidth and high sensitivity which accounts for the inevitable downshift introduced by biological tissues. Transmit pulse changes and software-based image filtering further improve penetration and maximum imaging depth. Imaging between 0 and 3 cm is still of higher quality, coincident with the PZ in all prostates [16], with progressive loss of lateral resolution and signal-to-noise ratio between 3 and 5 cm.

Biopsy procedure

All prostate biopsies were performed by two senior radiologists (F.C., A.L.) with 25 and 10 years of experience, respectively, in prostate MRI and TRUS-guided biopsies. Before microUS, diagnostic MR images were reviewed by the operator to re-localize and confirm the bp-MRI score of the lesion. The prostate was scanned in the parasagittal plane using microUS, and MRI findings in the sagittal plane were matched. For any MRI lesions visible on microUS, visually directed real-time microUS-guided targeted biopsy was performed (Figs. 1 and 2). Any visible homogenous or heterogenous hypoechoic focal lesion was considered suspicious on microUS. Risk classification scores, as proposed in the initial clinical report on microUS [16], were not assigned as part of this study. MRI+/microUS− lesions were biopsied using MRI-TRUS image fusion. T2-weighted and DWI images were loaded on the computer placed close to the TRUS equipment and processed using an open-source DICOM viewer (Weasis). A region of interest was placed on the lesion on T2-weighted and/or DW images, and a straight line was drawn parallel to the posterior aspect of the prostate on the sagittal plane. Images were then transferred to the ExactVu system. The probe was aligned along the midline (proximal and distal urethra), and the FusionVu software was activated to perform the reslicing necessary to make the MRI and microUS imaging planes match. The MR images and marked region of interest were displayed in a corner of the TRUS screen, allowing for real-time synchronization of the MRI and microUS volumes, but without MRI/microUS image overlay (Fig. 3). Image fusion was used when lesions were not visible or hardly visible on microUS (Fig. 3). All procedures were performed under light conscious sedation. The median number of cores taken during biopsy was 4 ± 2 (SD) (range, 2–10). Systematic biopsies were not performed in every patient and the decision was at the discretion of the operator.

Tumors were considered significant if there was any Gleason grade 4 component or any sample possessed a maximum cancer core length > 3 mm for Gleason 3 + 3 tumors according to University College London definition 1 [23]. The sensitivity and specificity of microUS were calculated on a per-lesion and per-patient basis, using the biopsy results as the reference standard.

Statistical analysis

Statistical analysis was performed using SPSS software (version 20.0, IBM). Quantitative variables were expressed as medians with first and third quartile and means ± SDs and ranges. Qualitative variables were expressed as raw numbers, proportions or frequency and percentages. Normality of distributions was assessed using histograms and the Shapiro-Wilk test. Comparisons were performed using the Student *t* test and Fisher or chi-square test. Significance was set at $p < 0.05$. The sensitivity and specificity of microUS to localize an MRI-targeted sPCa were calculated along with their 95% confidence intervals (CI) on a per-lesion and per-patient basis using binomial proportions.

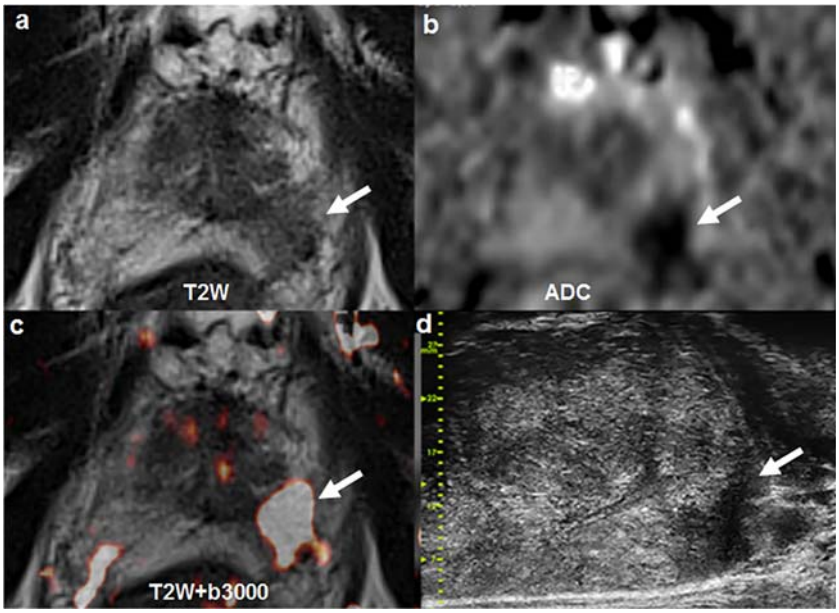

Fig. 1 Typical PZ bp-MRI score 4 lesion, left apex (arrow, **a**–**c**), in a 67-year-old man with a PSA level of 7 ng/mL. The corresponding image on microUS presents as a homogenous hypoechoic nodule (arrow, **d**). Targeted biopsy results: Gleason score 4 + 3 tumor; maximum cancer core length, 9 mm; 10% cribriform pattern

Results

Overall, 144 lesions were analyzed in the 118 patients (Table 3). The index lesion being a pathological definition, not applicable to MRI, the primary lesion for each patient was considered to be the lesion with the greatest long axis measured in the cranio-caudal plane, given the sagittal scanning used for microUS. Of the 144 lesions, 114 lesions (114/144, 79.2%) were visible on both MRI and microUS (MRI+/microUS+ lesions), 13 lesions (13/144, 9%) were visible on MRI but not visible on microUS (MRI+/microUS− lesions), and 17 lesions (17/144) were not visible on MRI and visible on microUS (MRI−/microUS+ lesions).

Of the 114 MRI+/microUS+ lesions, histopathological analysis from biopsy specimens showed significant PCa in 70 lesions (70/114; 61.4%). According to the bp-MRI score, the cancer detection rate for sPCa was 21% (4/19), 63.9% (39/61), and 79.4% (27/34) for bp-MRI scores 3, 4, and 5,

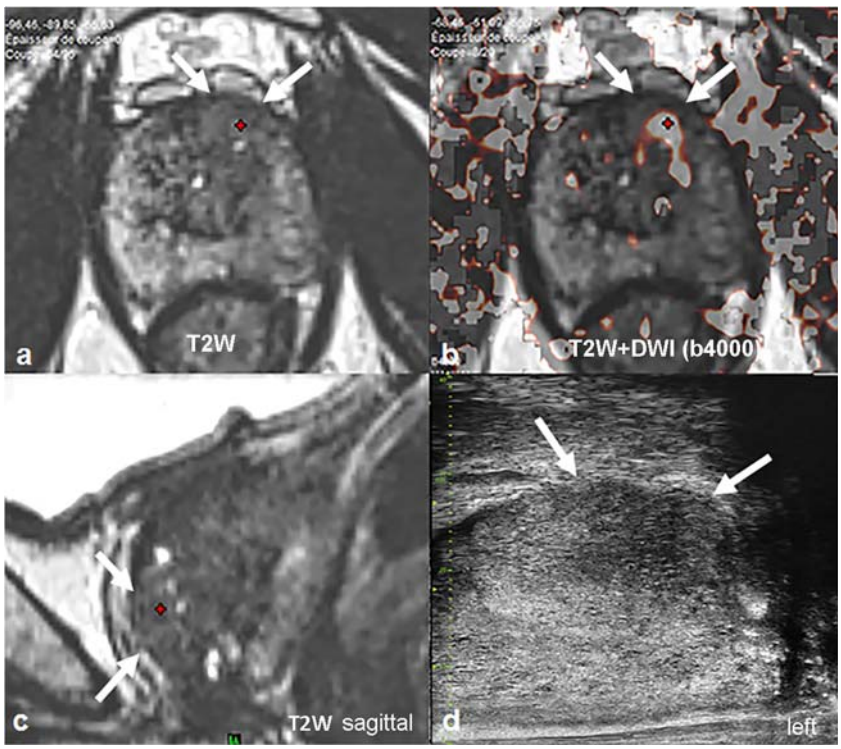

Fig. 2 Active surveillance for a Gleason 3 + 3 Ca detected by a set of 12 systematic biopsies (maximum cancer core length, 1 mm; left apex) in a 63-year-old with a rising PSA (8 ng/mL). A TZ apical focal area with restricted diffusion (arrows and red cross, **a**–**c**) is visible on bp-MRI. The corresponding hypoechoic area on microUS matches the MRI abnormality. Targeted biopsy results: Gleason 3 + 3 tumor; maximum cancer core length, 5 mm. Active surveillance was maintained

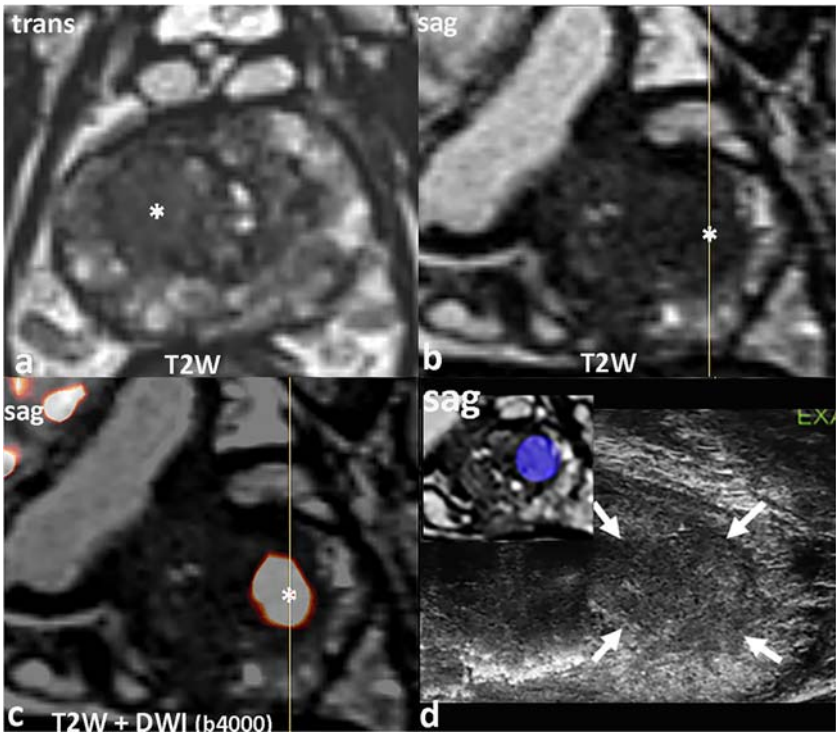

Fig. 3 Right TZ apical lesion with a bp-MRI score 5 (*, **a**–**c**) in a 64-year-old man with a PSA level of 8 ng/mL. The sagittal MRI views (**b**, **c**) have the same orientation as the microUS image (**d**). The lesion was barely visible on microUS. Image fusion was used, and real-time synchronization of microUS and MRI allowed to match with confidence the MRI lesion (blue tag) and the microUS lesion (arrows, **d**). Targeted biopsy results: Gleason score 3 + 4 tumor; maximum cancer core length, 10 mm; 0% cribriform pattern

respectively. Of the 24 TZ lesions involving the lower third of the TZ and within the field of exploration of microUS, 12 (12/24, 50%) were sPCa.

Of the 13 MRI+/ microUS− lesions (13/144, 9%), no sPCa was diagnosed by image fusion targeted biopsy. Eight lesions originated in the PZ (bp-MRI score 3, 4, and 5 in three, four, and one case, respectively). Four out of the five TZ lesions did not involve the apex (two in the midportion, one in the base, and one in the anterior fibromuscular stroma). On MRI, the mean size of these 13 lesions (12.6 mm ± 5.5 [SD]) was not significantly different from that of the 114 lesions visible on both modalities ($p = 0.29$) (Table 3).

Of the 17 MRI−/microUS+ lesions (17/144, 11.8%), four (4/17, 23.5%) were significant PCa. Two corresponded to the contralateral extension of the main lesion, not visible on MRI (Fig. 4) and two to a remote nodule (one ipsilateral and one contralateral) (Fig. 5). The mean cranio-caudal axis of these four lesions was 8 ± 2 (SD) mm (range, 4–10 mm) (Fig. 6), significantly smaller than that of the 114 tumors visible on both imaging modalities ($p < 0.0001$) (Table 3).

Overall, the cancer detection rate achieved by a second-look microUS-directed biopsy, performed after a biparametric MRI showing a lesion with a score > 2, was 57.6% (83/144; 95% CI, 49.1–65.8%) for any cancer and 51.4% (74/144; 95% CI, 42.9–59.8%) for sPCa. All 74 sPCa were visible on microUS, yielding 100% sensitivity (95% CI, 84.9–100%) and 22.8% specificity (95% CI, 12.5–35.8%) on a per-lesion basis, and 100% sensitivity (95% CI, 85.1–100%) and 22.6% specificity (95% CI, 12.3–36.2%) on a per-patient basis.

Discussion

In our study, all significant prostatic tumors visible on bp-MRI could be reidentified by microUS, used as a second-look imaging modality, given the known location of the lesion on bp-MRI. No other ultrasound technology has demonstrated such high sensitivity. The performance of conventional second-look ultrasound to detect PZ lesions was highlighted in previous reports [24–26]. Image fusion greatly increased the visibility of MRI lesions during ultrasound, achieving a detection rate of up to 88% for lesions originating in the PZ [26]. In one study [24], it was pointed out that second-look TRUS during image fusion with elastic co-registration was useful to avoid targeting errors inherent to virtual biopsy guidance. Using microUS guidance, the lesion targeted during biopsy is directly visible. The prostate is scanned in the sagittal plane with microUS, and detected lesions, especially when they are subtle, can be accurately matched with MRI findings displayed in the same plane. Visual matching is thus more accurate than during transrectal MRI-TRUS image fusion, in which TRUS images of a conventional end-fire transducer are acquired in an oblique plane and MR images are displayed in the axial plane [11]. In our study, it can be assumed that 100% sensitivity was achieved thanks to the very high spatial resolution of microUS and to the knowledge of the location of the MRI lesion. This rate is close to the sensitivity of 94% reported in the study by Lughezzani et al [17], in a microUS series of 104 patients with a visible

Table 3 Characteristics of the 144 lesions detected by microUS and/or MRI

All lesions *n* = 144	MRI+/microUS+ 114 (79.2%)	MRI+/microUS− 13 (9%)	MRI−/microUS+ 17 (11.8%)
Large-axis (mm)			
MicroUS			
Median (q1–q3)	12 (11–20)	n.a.	8 (4.75–8.5)
Mean ± SD [range]	14.1 ± 4.5 [8–27]	n.a.	8.1 ± 2.1 [4–12]
bp-MRI		11 (9–12)	
Median (q1–q3)	13 (11–20)	12.3 ± 5.5 [8–24]	n.a.
Mean ± SD [range]	14.2 ± 5.1 [8–25]		n.a.
Zone of origin			
PZ	86/114 (75.4%)	7/13 (54%)	17/17 (100%)
TZ	24/114 (21.1%)	6/13 (46%)	0/17 (0%)
CZ	4/114 (3.5%)	0/13 (0%)	0/17 (0%)
Significant PCa	70/114 (61.4%)	0/13 (0%)	4/17 (23.5%)
PZ	56/70 (80%)	0/13 (0%)	4/4 (100%)
TZ	12/70 (17%)	0/13 (0%)	0/4 (0%)
CZ	2/70 (3%)	0/13 (0%)	0/4 (0%)
Nonsignificant PCa	5/114 (4.4%)	2/13 (15%)	2/17 (12%)
PZ	2/5 (40%)	0/2 (0%)	2/2 (100%)
TZ	3/5 (60%)	2/2 (100%)	0/2 (0%)
Benign	39/114 (34.2%)	11/13 (85%)	11/17 (65%)
bp-MRI score			
3	19/114 (16.7%)	6/13 (46%)	n.a.
4	61/114 (53.5%)	6/13 (46%)	n.a.
5	34/114 (29.5%)	1/13 (8%)	n.a.

Quantitative variables are expressed as medians (numbers in parentheses are first and third quartiles) and means ± standard deviation [numbers in brackets are ranges]. Qualitative variables are expressed as raw numbers; numbers in parentheses are percentages

PZ peripheral zone, *TZ* transition zone, *CZ* central zone, *n.a.* not applicable

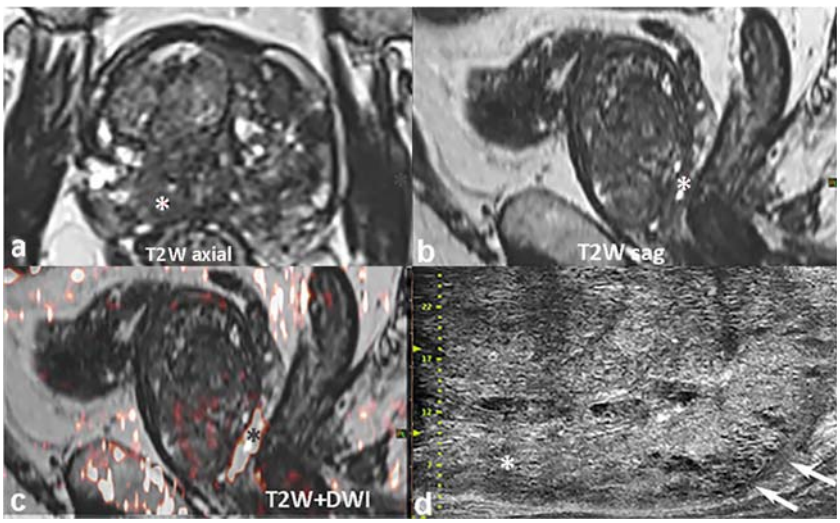

Fig. 4 Hypointense area with restricted diffusion (*, **a**–**c**) in a 73-year-old man with a PSA level of 33 ng/mL. MRI prostate volume is 110 cm^3. The lesion involves the right midportion and apex (17 mm) and was assumed to originate in the PZ and thus assigned a score 5. On microUS (**d**), the midportion of the PZ (*) did not show any focal lesion and the only finding in the lower apex was cystic atrophy (arrow, **d**). Image fusion-guided microUS biopsy of the apex and midportion revealed a single microfocus (1 mm) Gleason score 3 + 3. The MRI focal lesion was assumed to correspond to benign TZ tissue and the micro-carcinoma to a fortuitous diagnosis

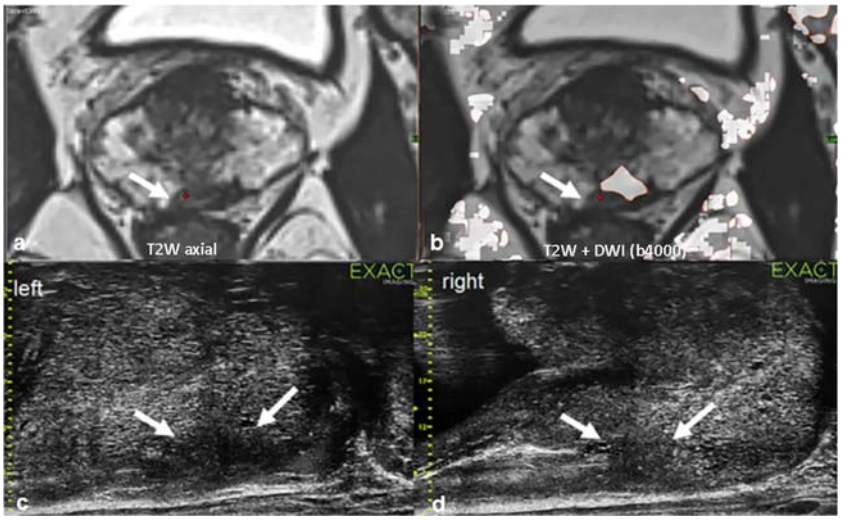

Fig. 5 Hypointense lesion with restricted diffusion, visible on bp-MRI and abutting the left central zone (**a**, **b**) in a 64-year-old man with a PSA level of 6 ng/mL. The contralateral hypointense area (white arrow and red cross) showed no restricted diffusion. MicroUS showed a left hypoechoic nodule (arrows, **d**) corresponding to the MRI lesion and a contralateral hypoechoic nodule (arrows, **d**). Both images were Gleason score 3 + 4 tumors with a maximum cancer core length of 8 and 5 mm, respectively, with 15% grade 4 and 0% cribriform pattern

lesion on mpMRI, whereas in the study by Ghai et al [16], microUS was performed as the primary imaging modality and yielded a lower sensitivity of 80%.

Conventional TRUS has a limited sensitivity to detect TZ tumors, even if TRUS is performed after MRI, in which case only some large-volume TZ tumors can be visualized [24]. We found that in a second-look setting tumors involving the lower third of the TZ, site of origin of most TZ tumors [27, 28], could be detected with 100% sensitivity by microUS. Indeed, the imaging depth of microUS is currently limited to 5 cm, which allows for best performance in the lower third of the prostate, where the anterior-posterior axis of the prostate is smaller than at the mid- or upper third portion. Thus, the very high spatial resolution of microUS provides clear benefit to detect TZ cancers within this region. The smallest TZ lesion of our series had a large axis of 8 mm. Our preliminary results thus show that TZ MRI-detected lesions with a cranio-caudal axis greater than 7 mm and originating in the lower third of the gland could be visualized by microUS with 100% sensitivity.

Our series also included 13 MRI+/microUS− prostatic lesions where image fusion software was used to guide the biopsy. In the PZ, no clear reason could be found to explain why the lesions were not visible on microUS. In the TZ, the location of these lesions was atypical, outside of the lower and anterior third of the TZ; this may explain why microUS failed to detect these lesions. MRI-TRUS image fusion was necessary to target these microUS-invisible lesions. Interestingly, no sPCa was detected in this group. These cases may be considered false-negative findings, related to a lack of accuracy of the fusion system, but if larger series confirm that they are true-negative findings, it may be possible to defer the currently recommended biopsy. Instead, these patients could be followed with repeated PSA sampling, bp-MRI, and microUS, at least for score 3 lesions.

The second objective of our study was to determine if microUS could detect lesions not visible on MRI (MRI −/microUS+ lesions). Our initial results include four small-size, albeit significant, satellite MRI−/microUS + tumors,

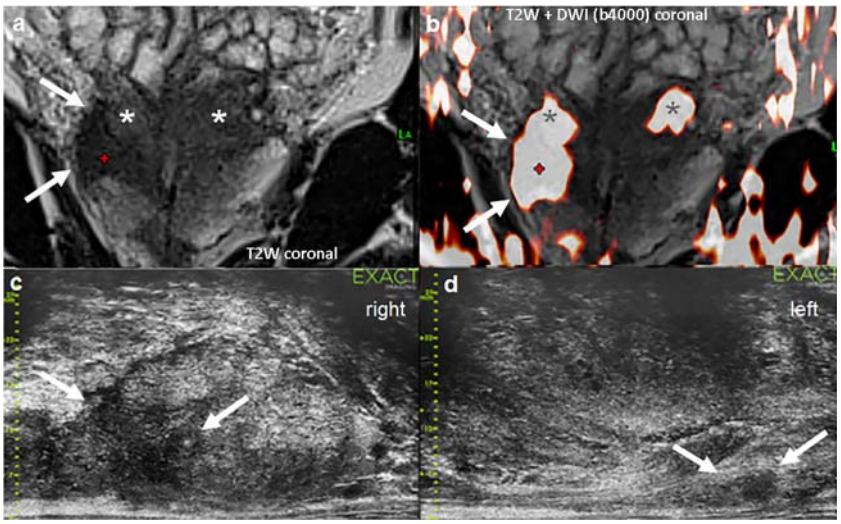

Fig. 6 Large lesion in the right PZ area on bp-MRI (arrows, **a**, **b**) in a 66-year-old man with a PSA level of 15 ng/mL. The lesion abuts the central zone (*), whose physiological restricted diffusion is well visible on the coronal view (*, **b**). MicroUS shows the right lesion corresponding to the MRI-visible lesion (arrow, **c**) and a contralateral nodule (arrows, **d**), remotely located from the main lesion, visible on MRI and not visible on bp-MRI. Targeted biopsies revealed that both lesions were Gleason score 4 + 4 tumors

two of them remotely located from the index lesion. This finding, noted in a recent article [15], highlights the potential of microUS for detecting significant small-volume tumors in patients with biologically suspected PCa, such as those with PSA density > 0.15 and non-suspicious MRI. According to a recent study by Panebianco et al [29], a 4-year follow-up of men with a non-suspicious MRI showed that in approximately 5% significant PCa remains non-visible and could only be detected by systematic biopsies [29]. Half of the tumors of this series contained a Gleason grade 4 component with a cribriform pattern, associated with poor prognosis [30]. Moreover, a study reported that only 26% of PZ and 20% of TZ tumors with a GS >3 + 4, but a tumor volume < 0.5 mL, were detected by multiparametric MRI [31]. To overcome this limitation, immediate targeted biopsy may be considered in patients with a biological suspicion of PCa and a positive microUS in a setting of a non-suspicious multi- or bp-MRI.

Our study has several limitations. First, it is not a randomized trial of other MRI fusion techniques versus second-look microUS, which would provide a higher level of evidence for the superiority of the second-look approach. Second, given the 5-cm depth limitation of the transducer, the sensitivity of microUS in the detection of lesions located in the TZ at the level of the middle third and the base of the prostate, as well as in the anterior stroma, remains to be demonstrated. Third, our study is a single-center study with a limited number of patients that does not allow definite conclusions to be drawn on whether MRI-directed high-frequency TRUS-guided biopsies can replace TRUS-MRI image fusion-guided biopsies. Further studies with more case material are needed to confirm our preliminary results.

In conclusion, our early single-center experience shows that microUS, used as a second-look examination with the knowledge of the location of the suspicious lesion on MRI, may show promise for targeting biopsies of all PZ lesions and TZ lesions originating in the lower third of the TZ. The value of microUS and MRI/microUS image fusion for the upper portion of the TZ and the anterior fibromuscular stroma, as well as the significance of discordant results between MRI and microUS findings, must be evaluated in a larger number of patients.

Funding information The authors state that this work has not received any funding.

Compliance with ethical standards

Guarantor The scientific guarantor of this publication is Dr. François Cornud.

Conflict of interest The authors declare that they have no competing interests.

Statistics and biometry No complex statistical methods were necessary for this paper.

Informed consent Written informed consent was waived by the Institutional Review Board.

Ethical approval Institutional Review Board approval was obtained.

Methodology
- retrospective
- observational
- performed at one institution

References

1. Kasivisvanathan V, Rannikko AS, Borghi M et al (2018) MRI-targeted or standard biopsy for prostate-cancer diagnosis. N Engl J Med 378:1767–1777
2. Rouviere O (2016) Will all patients with suspicion of prostate cancer undergo multiparametric MRI before biopsy in the future? Diagn Interv Imaging 97:389–391
3. Gorin MA, Walsh PC (2018) Magnetic resonance imaging prior to first prostate biopsy-are we there yet? Eur Urol 74:409–410
4. Ploussard G, Borgmann H, Briganti A et al (2018) Positive pre-biopsy MRI: are systematic biopsies still useful in addition to targeted biopsies? World J Urol 37:243–251
5. Garcia Bennett J, Vilanova JC, Guma Padro J, Parada D, Conejero A (2017) Evaluation of MR imaging-targeted biopsies of the prostate in biopsy-naive patients: a single centre study. Diagn Interv Imaging 98:677–684
6. Villers A, Marliere F, Ouzzane A, Puech P, Lemaitre L (2012) MRI in addition to or as a substitute for prostate biopsy: the clinician's point of view. Diagn Interv Imaging 93:262–267
7. Pokorny MR, de Rooij M, Duncan E et al (2014) Prospective study of diagnostic accuracy comparing prostate cancer detection by transrectal ultrasound-guided biopsy versus magnetic resonance (MR) imaging with subsequent MR-guided biopsy in men without previous prostate biopsies. Eur Urol 66:22–29
8. Delongchamps NB, Lefèvre A, Bouazza N, Beuvon F, Legman P, Cornud F (2015) Detection of significant prostate cancer with magnetic resonance targeted biopsies–should transrectal ultrasound-magnetic resonance imaging fusion guided biopsies alone be a standard of care? J Urol 193:1198–1204
9. Yarlagadda VK, Lai WS, Gordetsky JB et al (2018) MRI/US fusion-guided prostate biopsy allows for equivalent cancer detection with significantly fewer needle cores in biopsy-naive men. Diagn Interv Radiol 24:115–120
10. Cornud F, Roumiguie M, Barry de Longchamps N et al (2018) Precision matters in MR imaging-targeted prostate biopsies: evidence from a prospective study of cognitive and elastic fusion registration transrectal biopsies. Radiology 287:534–542
11. Cornud F, Brolis L, Delongchamps NB et al (2013) TRUS-MRI image registration: a paradigm shift in the diagnosis of significant prostate cancer. Abdom Imaging 38:1447–1463
12. Ukimura O, Desai MM, Palmer S et al (2012) 3-Dimensional elastic registration system of prostate biopsy location by real-time 3-dimensional transrectal ultrasound guidance with magnetic resonance/transrectal ultrasound image fusion. J Urol 187:1080–1086
13. Cornud F, Bomers J, Futterer JJ, Ghai S, Reijnen JS, Tempany C (2018) MR imaging-guided prostate interventional imaging: ready for a clinical use? Diagn Interv Imaging 99:743–753
14. Barral M, Lefevre A, Camparo P et al (2019) In-bore transrectal MRI-guided biopsy with robotic assistance in the diagnosis of prostate cancer: an analysis of 57 patients. AJR Am J Roentgenol 213:171–179

15. Abouassaly R, Klein EA, El-Shefai A, Stephenson A (2019) Impact of using 29 MHz high-resolution micro-ultrasound in real-time targeting of transrectal prostate biopsies: initial experience. World J Urol. https://doi.org/10.1007/s00345-019-02863-y
16. Ghai S, Eure G, Fradet V et al (2016) Assessing cancer risk on novel 29 MHz micro-ultrasound images of the prostate: creation of the micro-ultrasound protocol for prostate risk identification. J Urol 196:562–569
17. Lughezzani G, Saita A, Lazzeri M et al (2019) Comparison of the diagnostic accuracy of micro-ultrasound and magnetic resonance imaging/ultrasound fusion targeted biopsies for the diagnosis of clinically significant prostate cancer. Eur Urol Oncol 2:329–332
18. Pavlovich CP, Cornish TC, Mullins JK et al (2014) High-resolution transrectal ultrasound: pilot study of a novel technique for imaging clinically localized prostate cancer. Urol Oncol 32:34.e27–34.e32
19. Engels RRM, Israel B, Padhani AR, Barentsz JO (2019) Multiparametric magnetic resonance imaging for the detection of clinically significant prostate cancer: what urologists need to know. Part 1: acquisition. Eur Urol. https://doi.org/10.1016/j.eururo.2019.09.021
20. Pierre T, Cornud F, Colleter L et al (2017) Diffusion-weighted imaging of the prostate: should we use quantitative metrics to better characterize focal lesions originating in the peripheral zone? Eur Radiol 28:2236–2245
21. Rosenkrantz AB, Parikh N, Kierans AS et al (2016) Prostate cancer detection using computed very high b-value diffusion-weighted imaging: how high should we go? Acad Radiol 23:704–711
22. Rosenkrantz AB, Kim S, Campbell N, Gaing B, Deng FM, Taneja SS (2015) Transition zone prostate cancer: revisiting the role of multiparametric MRI at 3 T. AJR Am J Roentgenol 204:W266–W272
23. Ahmed HU, Hu Y, Carter T et al (2011) Characterizing clinically significant prostate cancer using template prostate mapping biopsy. J Urol 186:458–464
24. Ukimura O, Marien A, Palmer S et al (2015) Trans-rectal ultrasound visibility of prostate lesions identified by magnetic resonance imaging increases accuracy of image-fusion targeted biopsies. World J Urol 33:1669–1676
25. van de Ven WJ, Sedelaar JP, van der Leest MM et al (2016) Visibility of prostate cancer on transrectal ultrasound during fusion with multiparametric magnetic resonance imaging for biopsy. Clin Imaging 40:745–750
26. van de Ven WJ, Venderink W, Sedelaar JP et al (2016) MR-targeted TRUS prostate biopsy using local reference augmentation: initial experience. Int Urol Nephrol 48:1037–1045
27. Chesnais AL, Niaf E, Bratan F et al (2013) Differentiation of transitional zone prostate cancer from benign hyperplasia nodules: evaluation of discriminant criteria at multiparametric MRI. Clin Radiol 68:e323–e330
28. Tavolaro S, Mozer P, Roupret M et al (2018) Transition zone and anterior stromal prostate cancers: evaluation of discriminant location criteria using multiparametric fusion-guided biopsy. Diagn Interv Imaging 99:403–411
29. Panebianco V, Barchetti G, Simone G et al (2018) Negative multiparametric magnetic resonance imaging for prostate cancer: what's next? Eur Urol 74:48–54
30. Kweldam CF, Kummerlin IP, Nieboer D et al (2017) Presence of invasive cribriform or intraductal growth at biopsy outperforms percentage grade 4 in predicting outcome of Gleason score 3+4=7 prostate cancer. Mod Pathol 30:1126–1132
31. Vargas HA, Hotker AM, Goldman DA et al (2016) Updated prostate imaging reporting and data system (PIRADS v2) recommendations for the detection of clinically significant prostate cancer using multiparametric MRI: critical evaluation using whole-mount pathology as standard of reference. Eur Radiol 26:1606–1612